Archives of Oral Biology (2005) **50**, 843–848

Available online at www.sciencedirect.com

SCIENCE DIRECT®

Archives of Oral Biology

www.intl.elsevierhealth.com/journals/arob

Characterization of enamel with variable caries risk

Pilar Gutierrez [a], Cristina Piña [a], Victor Hugo Lara [b], Pedro Bosch [a,*]

[a] *Instituto de Investigaciones en Materiales, Universidad Nacional Autónoma de México, Circuito Exterior, Ciudad Universitaria, 04510 México, D.F., Mexico*
[b] *Departamento de Química, Universidad Autónoma Metropolitana-Iztapalapa, Michoacán y La Purísima, Iztapalapa, 09340 México, D.F., Mexico*

Accepted 17 November 2004

KEYWORDS
Enamel;
Caries risk;
Hydroxyapatite;
Fractal dimension;
Tooth;
FTIR;
XRD;
SAXS

Summary Small angle X-ray scattering (SAXS), X-ray diffraction (XRD), and Fourier transform infrared spectroscopy (FTIR) have been used to look at enamel from nine premolars, three each from individuals in low, medium and high risk caries groups. Only SAXS was able to detect consistent differences between any of the groups. In enamel from the high caries risk group, the micropores between the hydroxyapatite crystals were laminar. In enamel from the low caries risk group, the micropores were cylindrical. Other parameters varied between teeth but were not correlated with caries risk.

Introduction

The susceptibility to caries varies between individuals.[1] Large scale epidemiological studies in children show that 50% are caries free, 25% have 25% of the lesions and 25% have 75% of the total number of lesions.[2–6] This has led to the recognition of three levels of susceptibility, low, medium and high.[3] The structural/compositional basis of this variation is unknown. Differences in enamel hardness have been described,[7] differences in hydroxyapatite crystal orientation may also occur but the currently available data are inconclusive.[8]

A new technique, small angle X-ray scattering (SAXS), has recently become available to examine hard tissue. SAXS has been already used to characterize dentin[9,10] and bone.[11,12] This approach allows the detection of inhomogeneities such as protein inclusions, voids and micropores. We have combined this approach with X-ray diffraction (XRD) and Fourier transform infrared spectroscopy (FTIR) to examine structure, pore size & shape and the presence of carbonate in teeth from individuals in all three levels of risk.

Materials and methods

Samples

Nine children all 14-years-old but with range of susceptibilities to caries were selected from patients undergoing premolar extractions as part of orthodontic treatment.

* Corresponding author. Tel.: +56 22 46 56.
E-mail address: croqcroq@hotmail.com (P. Bosch).

0003-9969/$ – see front matter
doi:10.1016/j.archoralbio.2004.11.018

For the purposes of this study high caries risk (HCR) was defined as having four or more lesions at least one of which extended beyond the oclusal surface. Medium caries risk (MCR) was defined as having three or few carious lesions none which extended beyond the occlusal surface. Low risk caries (LCR) was defined as caries free. Three patients in each group were chosen.[13] The protocol was approved by the ethics committee of the biomaterials disposal of the UNAM and the teeth were used with the written consent of both child and parents.

Premolar teeth were obtained from three children in each of the three groups. The crown was removed from each tooth and smooth, defect free areas selected under a stereoscopic microscope. Enamel from these areas was powdered and examined by three techniques.

Conventional powder X-ray diffraction (XRD)

Conventional diffraction patterns were obtained with a Bruker AXS, D8 Model Advance diffractometer coupled to a copper anode X-ray tube (Kα radiation). Compounds were identified using the JCPDS files. To determine hydroxyapatite cell parameters, a NaCl internal standard was introduced and the peaks were measured in the interval 21—29°(2θ).

Infrared spectroscopy (FTIR)

A FTIR spectrometer Nicolet, model 510P, was used. Samples were compacted into KBr pellets and the analysis was by direct transmission to identify the carbonate radicals as these have been often linked to the caries risk.[14,15]

Small angle X-ray scattering (SAXS)

A Kratky camera coupled to a copper anode tube was used to measure the SAXS curves. The distance between the sample and the linear proportional counter was 25 cm; a Ni filter selected the copper Kα radiation. The sample was introduced into a capillary tube. The intensity $I(h)$ was measured for 9 min in order to obtain good quality statistics.

The SAXS data were processed with the ITP program[16—20] where the angular parameter (h) is defined as $h = 4\pi\sin(\theta/2)/\lambda$, where θ and λ are the X-ray scattering angle and wavelength, respectively. The radius of gyration (R_g) could, then, be obtained from the slope of the Guinier plot, Log $I(h)$ against h^2,[21] in the zone 1×10^{-3} Å$^{-2} < h^2 < 7 \times 10^{-3}$ Å^{-2}.

By the Babinet principle, the small angle X-ray scattering may be due either to dense particles in a low density environment or to pores or low density inclusions in a high electron density medium. As the hydroxyapatite crystals are large, beyond the range of sizes studied by SAXS, they do not cause scattering. Thus, the observed small dispersive entities must be closed or open micropores.

The shape of the scattering objects, in this case micropores, was estimated from the Kratky plot, i.e., $h^2\ I(h)$ against h. The shape of the pores is determined from the Kratky curve shape, then, for instance, if the curve presents a peak the pores are globular (bubbles).[22] If a pore shape can be determined,[18] the distance distribution function, i.e., the size distribution function, may be calculated.

It is also possible to estimate, from the slope of the curve Log $I(h)$ versus Log (h), the fractal dimension of the scattering objects[23,24] to determine whether the electron density changes are abrupt or smooth. For this study the background obtained with the Porod plot was substracted from the experimental intensity. The h interval was $0.07 < h < 0.18$ Å^{-1}.

Results

Fig. 1 shows the X-ray diffraction patterns of the enamel samples whose sharp and well defined peaks correspond to hydroxyapatite. Fig. 2 compares the hydroxyapatite (2 1 0) peak positions referred to an internal standard, in this work NaCl: The corresponding a-cell parameter value was found to vary from 9.44 to 9.51 Å, showing that some ion exchange, substitution or defects are present in this

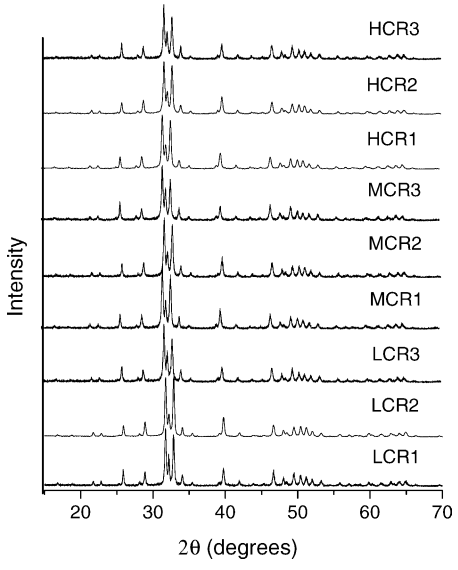

Figure 1 Comparison of the X-ray diffraction patterns of the various samples. All samples presented sharp and well defined peaks corresponding to hydroxyapatite.

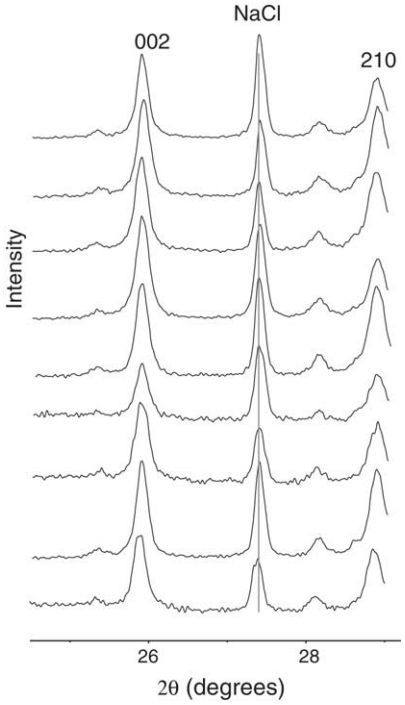

Figure 2 Comparison of the hydroxyapatite (2 1 0) and (2 0 0) peak positions referred to the NaCl peak. The diffraction pattern of the samples show not shift in the peak positions. The peak at 27.5°2θ corresponds to the internal standard NaCl.

direction. As in some samples the (2 1 0) peak was double, we report the two corresponding *a*-cell parameters, each one obtained from each maximum. The *c*-cell parameter was determined from the (0 0 2) peak and the obtained value was the same in all samples, Table 1. Although the *a*-cell parameter variations must be due to differences in hydroxyapatite composition, these variations were not related to caries risk.

Fig. 3 shows the FTIR spectrum of only one of the nine enamel samples as they are all identical, no

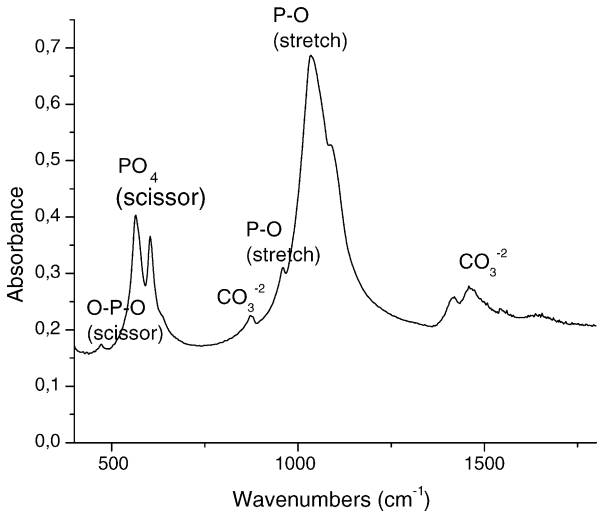

Figure 3 Infrared spectrum of one of the enamel samples.

correlation between infrared bands and caries susceptibility could be established. The small band found at 470 cm^{-1} can be attributed to an O-P-O scissor vibration. The expected scissor vibrations of PO_4^{-3} radicals are found at 525—610 cm^{-1} as a double peak. CO_3^{2-} vibrates at 840—890 cm^{-1}. At 954 a P-O stretching band is found. The band 1030—1090 corresponds to the stretching vibration of P-O. The broad band from 1400 to 1500 is due to carbonates (stretching and elongation of CO_3^{2-}). Lastly, the band at 3330—3450 cm^{-1} corresponds to hydroxyls not included in the figure.

Table 2 presents the radii of gyration, the shapes and the fractal dimensions obtained with SAXS. Although, the differences in fractal dimension, 2.2—2.9 are significant they have to be attributed to the organic material adhered to the hydroxyapatite crystals, indeed hydroxyapatite crystals are not fractal structures. This organic material partially fills the pores. The values obtained for gyration radii

Table 1 Hydroxyapatite cell parameters obtained from the X-ray diffraction patterns.

Sample	*a*-Cell parameter from peak 2 1 0 (Å)	*c*-Cell parameter from peak 0 0 2 (Å)
LCR1	9.46	6.88
LCR2	9.44 and 9.48	6.88
LCR3	9.46	6.88
MCR3	9.46 and 9.44	6.88
MCR2	9.45 and 9.48	6.88
MCR1	9.45 and 9.51	6.88
HCR1	9.46 and 9.45	6.88
HCR2	9.46	6.88
HCR3	9.46	6.88

Table 2 Comparison of gyration radii (R_g), fractal dimensions (D_f) and shapes of the pores and gaps as determined by small angle X-ray scattering (SAXS).

Sample	D_f	R_g (Å)	Shape
LCR1	2.4	53.2	Cylindrical
LCR2	2.4	51.7	Cylindrical
LCR3	2.6	51.2	Cylindrical
MCR1	2.9	54.0	Cylindrical
MCR2	2.9	54.0	Cylindrical
MCR3	2.9	54.0	Laminar
HCR1	2.3	49.0	Laminar
HCR2	2.2	55.0	Laminar
HCR3	2.2	50.2	Laminar

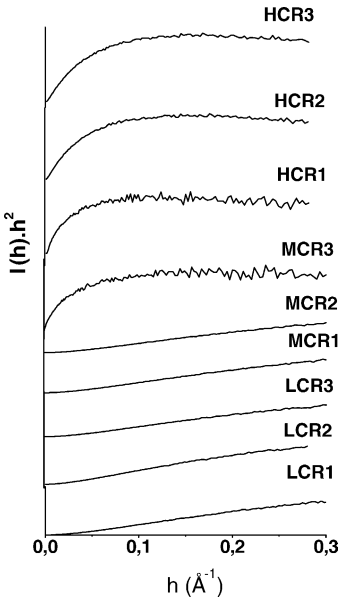

Figure 4 Kratky plot of three low risk, three medium risk and three high risk samples.

are similar within error range. Gyration radius is related to the mean pore size independently of the shape. From the Kratky plots, Fig. 4, the shape of the pores was established to be either cylindrical or laminar. In this case, a clear difference between the high and the low risk samples was established. Nevertheless, in the medium risk group the shape features are both, cylindrical or laminar, showing that shape is not the only factor in caries risk. Hence, thereafter, we chose to compare only the high and low risk results.

Assuming laminar pores in high caries risk samples and cylindrical pores in low risk samples, the corresponding size distribution functions were determined, Fig. 5. The size distribution functions in the low risk samples is broad. In two of the samples (LCR1 and LCR3), the maximum is found at about 60 Å in diameter but the sizes may vary from 10 to 80 Å. The size distribution function of the third low risk sample (LCR2) is also very broad, it presents two maxima corresponding to diameters of 30 and 120 Å. The particle size distribution functions of high risk samples show a bimodal function with pores whose thickness is 20—50 Å and 80—100 Å.

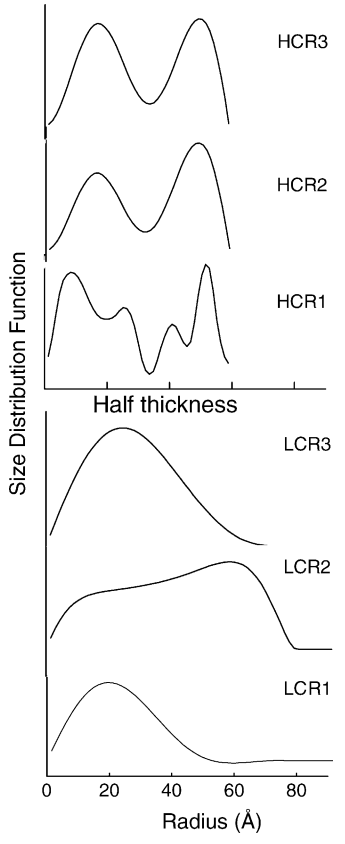

Figure 5 Pore size distribution of low and high risk enamel samples.

Discussion

Three different techniques DRX, FTIR and SAXS were used to characterize the enamel from low, medium and high caries risk patients. It has to be emphasized that our conclusions are qualitative, the selection of the samples corresponds to very specific patients whose characteristics in susceptibility to caries are extreme and whose statistical validity has been established by other authors.[7,13] X-ray diffraction showed that natural hydroxyapatite is the main component of enamel, as expected; no other compounds were observed. To identify a compound with this technique, it has to be constituted by rather large crystals (larger than 30 Å) and the amount has to be 3% or more. High and low risk caries samples could not be differentiated by their cell parameters.

Hydroxyapatite is known to exchange ions with the surrounding solutions. If such is the case, the a-cell parameter is modified. LeGeros et al.[15] found a higher a-cell parameter value for surface enamel apatite if compared with the value obtained from the inner enamel layers as carbonate and magnesium content increased. The reported values were 9.449, 9.445 and 9.440 Å for the outer, the middle and the inner layers of enamel. Our values are in the same range.

Two of the *a*-cell parameter values reported in this work show that a fraction of enamel was ion exchanged. The incorporation of carbonate ions to the hydroxyapatite structure has been proposed to explain the caries susceptibility as it seems to cause a diminution of crystal size and, therefore, an increased solubility.[14,15] However, we were not able

to identify the exchanged ions as FTIR spectra are all identical. The absorbance of the carbonate radical is at 1545 cm^{-1} and at 1415 cm^{-1} depending on the occupied site in the hydroxyapatite network.[15] The carbonate peak intensities remain constant in all our samples, therefore the carbonate amount does not vary. Thus, the variations in our cell parameters must be due to other substitutions or exchanges, fluorine for instance.

SAXS is due to the electron density difference between hydroxyapatite crystals and pores. In this case, as the diffraction peaks did not show any broadening, the hydroxyapatite crystals are very large and then the measured entities correspond to pores in enamel.[25–28] In the zone of the SAXS curves where the gyration radii were estimated no relevant differences within error range were observed. Thus, the pores between crystals have a similar mean size, without any assumption on the shape.

Differences in fractal dimensions were found, the medium caries risk samples showing the highest values (2.9). Hydroxyapatite is not a fractal compound and the expected value, if the pores are clean and neat, is 3. Instead, a value as low as 2.2 was found in the group of high caries risk samples. It seems that the pore walls in this case are not neatly defined, meaning that some organic compounds may be adhered. In the low risk samples the value 2.4 indicates the same. Then, fractal dimension has to be referred to the connectivity between pores due to the amount of adhered organic material (proteins) to the pore walls which, in turn, does not depend on the caries risk. In this sense, it is interesting to note that the medium caries risk samples are those that presented the double (0 0 2) diffraction peaks but this correlation has to be discarted as samples HCR1 and LCR2 present double diffraction peaks and low fractal dimension.

The Kratky plots are most relevant as they provide a clear evidence of the difference in pore shape and such difference can be correlated with the caries risk. If pores are cylindrical the caries risk is low but, if they are laminar, the risk is high, Table 2. The medium risk samples present an intermediate situation which turns out to be either closer to the low risk samples as in samples MCR1 and MCR2 (cylindrical pores) or to the high risk samples as in MCR3 (laminar pores).

Most probably, the crystalline faces exposed to acids vary depending on the shape of the pore, of course laminar pores tend to expose preferentially one of the hydroxyapatite crystalline planes. Such correlation is independent of the fractal dimension values which in turn may correspond as already discussed to the degree of connectivity among the pores due to the amount of adhered organic material. Only the shape of the pores is determinant. This correlation is in agreement with the determined pore size distribution functions which are definitely different in high risk and low risk samples. Note that these distributions measure different parameters, if laminar pores are assumed they correspond to the thickness of the pore but, if cylindrical pores are assumed, they correspond to the diameter of such cylinders. Even if the number of studied samples is small the results are reproducible and all the high risk samples behave in the same way. The results are encouraging and are the first step to a more detailed study of caries risk and enamel pores.

Although dentin and enamel are very different in the mineral/organic phases organization, the thickness of the scattering objects reported by Tesch et al.[9] for dentin are relevant to us. These authors found that the thickness of their scattering objects in SAXS was the best predictor for hardness and elastic modulus, better even than the mineral content. The values for thickness were 23—36 Å, and although they advice that these values cannot be compared to the dentin apatite crystal thickness measured previously by TEM (103 Å), they attribute them to small mineral particles. We believe that these measurements (23—36 Å) correspond, as ours, to pores between the apatite crystals.

Conclusion

Conventional techniques as X-ray diffraction or infrared spectroscopy were not able to distinguish between enamels with high caries risk and the corresponding low risk samples, although the cell parameters of hydroxyapatite varied. SAXS technique was able to establish the size and the shape of the pores among the apatite crystals. This shape, cylindrical or laminar, should determine the crystalline faces exposed to environment (saliva, acids, ...). Furthermore, depending on the exposed crystalline faces, the attack could be more or less pronounced, i.e. the tooth would be more or less caries susceptible. More work will be required to clarify this issue. Last but not least, these features could determine the resistance of the material,[29] but remains to be determined why the high caries risk patients develop laminarly shaped pores.

Acknowledgements

The technical work of Leticia Baños, Miguel Angel Canseco and Carlos Flores is gratefully acknowledged.

References

1. Mandel ID. Nature versus nurture in dental caries. *J American Dental Assoc* 1994;**125**:1345—51.
2. Hausen H, Kärkkäinen S, Seppä L. Application of high risk strategy to control dental caries. *Community Dent Oral Epidemiol* 2000;**28**:26—34.
3. Burt BA. Prevention policies in the light of changed distribution of dental caries. *Acta Odontol Scan* 1998;**56**: 179—86.
4. Bjarnason S, Finnbogason SY, Holbrook P, Kohler B. Caries experience in Icelandic 12-year-old urban children between 1984 and 1991. *Community Dent Oral Epidemiol* 1993;**21**: 195—7.
5. Mosha HJ, Fejerskov O, Langebaek J, Thylstrup A, Baelum V, Manji F. Caries experience in urban Tanzania children 1973—84. *Scan J Dent Res* 1988;**96**:385—9.
6. Wei SH, Holm AK, Tong LS, Yuen SW. Dental caries prevalence and related factors in 5-year-old children in Hong Kong. *Pediatr Dent* 1993;**15**:119—23.
7. Gutiérrez-Salazar MP, Reyes-Gasga J. Enamel hardness and caries susceptibility in human teeth. *Revista Latinoamericana de Metalurgia y Materiales* 2001;**21**:36—40.
8. Cevč G, Cevč P, Schasra M, Skaleric U. The caries resistance of human teeth is determined by the spatial arrangement of hydroxyapatite microcrystals in enamel. *Nature* 1980; **286**:425—7.
9. Tesch W, Eidelman N, Roschger P, Goldenberg F, Klaushofer K, Fratzl P. Graded microstructure and mechanical properties of human crown dentin. *Calcif Tissue Int* 2001;**69**:147—57.
10. Kinney JH, Pople JA, Marshall GW, Marshall SJ. Collagen orientation and crystallite size in human dentin: a small angle X-ray scattering study. *Calcif Tissue Int* 2001;**69**: 31—7.
11. Fratzl P, Groschner M, Vogl G, Plenk H, Eschberger JR, Fratzl-Zelman N, et al. Mineral crystals in calcified tissue: a comparative study by SAXS. *J Bone Miner Res* 1992;**7**:329—34.
12. Fratzl P, Fratzl-Zelman N, Klaushofer K, Volg G, Koller K. Nucleation and growth of mineral crystals in bone studied by small-angle X-ray scattering. *Calcif Tissue Int* 1991;**48**: 407—13.
13. Burchel CK, Stephen KW, Schäfer F, Huntington E. Improved sensitivity in caries clinical trials by selection on basis of baseline caries experience. *Community Dent Oral Epidemiol* 1991;**19**:20—2.
14. Weatherell JA, Robinson G, Hallsworth AS. Variations in chemical composition of human enamel. *J Dent Res* 1974; **53**:180—92.
15. LeGeros RZ, Sakae T, Bautista C, Retino M, LeGeros JP. Magnesium and carbonate in enamel and synthetic apatites. *Adv Dent Res* 1996;**10**:225—31.
16. Glatter O. Convolution square root of band-limited symmetrical functions and its application to small-angle X-ray scattering. *J Appl Cryst* 1981;**14**:101—8.
17. Glatter O. Comparison of two different methods for direct structure analysis from small angle X-ray scattering data. *J Appl Cryst* 1988;**21**:886—90.
18. Glatter O. Scattering studies on colloids of biological interest (amphiphilic systems). Progress in Colloid and Polymer. *Science* 1991;**84**:46—54.
19. Glatter O, Hainisch B. Improvements in real-space deconvolution of small angle scattering data. *J Appl Cryst* 1984; **17**:435—41.
20. Glatter O, Gruber K. Indirect transformation in reciprocal space: desmearing of small-angle scattering data from partially ordered systems. *J Appl Cryst* 1993;**26**:512—8.
21. Guinier A, Fournet G. *Small-angle scattering of X-rays*. New York: John Wiley & Sons Inc; 1955.
22. Kataoka M, Flanagan JM, Tokunaga F, Engelman DM. Use of X-ray solution scattering for protein folding study. In: Chanse B, Deisenhofer J, Ebashi S, Goodhead DT, Huxley HE, editors. *Synchrotron radiation in the biosciences*. Oxford, UK: Clarendon Press; 1994. p. 87—92.
23. Harrison A. *Fractals in chemistry*. New York: Oxford University Press Inc.; 1995. p. 47—65.
24. Martin JE, Hurd AJ. Scattering from fractals. *J Appl Cryst* 1987;**20**:61—78.
25. Gwinnett AJ. Normal enamel I. Quantitative polarized light study. *J Dent Res* 1966;**45**:120—7.
26. Dibdin GH, Poole DFG. Surface area and pore size analysis for human enamel and dentin by water vapour sorption. *Arch Oral Biol* 1982;**27**:235—41.
27. Shellis RP. A scanning electron-microscopic study of solubility variations in human enamel and dentine. *Arch Oral Biol* 1996;**41**:473—84.
28. Shellis RP. Relationship between human enamel structure and the formation of caries-like lesions in vitro. *Arch Oral Biol* 1984;**29**:975—81.
29. Popowics TE, Rensberger JM, Herring SW. Enamel microstructure and microstrain in the fracture of human and pig molar cusp. *Arch Oral Biol* 2004;**49**:595—605.